Gas–liquid chromatography–mass spectrometry of trimethylsilyl ethers of bile alcohols

G. S. Tint, B. Dayal, A. K. Batta, S. Shefer, F. W. Cheng, G. Salen, and E. H. Mosbach

Gastroenterology Section, Veterans Administration Hospital, East Orange, NJ 07019; Department of Medicine, College of Medicine and Dentistry, New Jersey Medical School, Newark, NJ 07103; Public Health Research Institute of The City of New York, Inc., NY 10016; and the Cabrini Health Care Center, New York, NY 10003.

Abstract This report describes the gas–liquid chromatography–mass spectrometry (GLC–MS) of the trimethylsilyl ethers of 5β-cholestane-3α,7α,12α-triol with mono- or dihydroxy substitution in the side chain. Compounds with 24- and 25-unsaturation in the side chain were also studied. The gas–liquid chromatographic separation of the different bile alcohols was carried out using 3% QF-1 and 1% HI-EFF 8BP as column packings. Both columns were useful in that the retention times of the trimethylsilyl ethers of the various 5β-cholestanetetrols varied linearly with the position of the side-chain trimethylsiloxyl substituent. The major fragmentations in the GLC–MS of all bile alcohols tested were due to the trimethylsiloxyl side-chain substituent(s). A trimethylsiloxyl group at C-22 was the most effective in promoting side-chain fragmentation, followed, in order of decreasing effectiveness, by substituents at carbons 25, 23, 24, and 26. The side-chain fragments generally gave rise to one or two intense mass peaks and a series of weaker peaks, 90 mass units apart, owing to the loss of successive molecules of trimethylsilanol. Most 5β-cholestane-triols, -tetrols, and -pentols can be unequivocally identified by their strong side-chain fragmentation peaks, except for 5β-cholestane-3α,7α,12α,26-tetrol, the trimethylsilyl ether of which exhibited very low intensity side-chain fragments.

Supplementary key words electron impact mass spectrometry · C_{27}-bile alcohols.

Bile alcohols are the immediate evolutionary predecessors of bile acids (1, 2). These polyhydroxy steroids are the main constituents in the bile of certain reptiles, primitive bony fishes, sharks, and rays (1–4), but can also be detected in the bile of higher animals (5–7). Furthermore, bile alcohols are known to be intermediates in the biosynthesis of the two primary bile acids, cholic acid and chenodeoxycholic acid, by mammalian liver (6). It is in this latter role that they have attained renewed interest. Recent investigations into the mechanism by which the sterol side chain is hydroxylated during the synthesis of bile acids from cholesterol (8–15) have created the need for adequate methodology for the characterization and identification of bile alcohols.

This report deals with gas–liquid chromatography–mass spectrometry (GLC–MS) of the trimethylsilyl (TMS) ethers of a number of 5β-cholestanetriols, -tetrols, and -pentols all having nuclear hydroxy substituents at the 3α, 7α, and 12α positions. Its main purpose is to provide diagnostic tools for identification and characterization of these compounds and to aid in the interpretation of the side-chain fragmentation patterns.

METHODS

Gas–Liquid chromatography (GLC)

To prepare the TMS ethers, the individual bile alcohols (100 μg) were mixed with 70 μg of 5α-cholestane and were treated with 100 μl of Sil-Prep (Applied Science Labs., State College, PA) for 30 min at 45°C. Retention times relative to 5α-cholestane were measured on a Hewlett-Packard Model 7610A gas chromatograph equipped with flame ionization detectors, and a Model CRS-204 timer–integrator (Columbia Scientific Industries, Austin, TX). Silanized U-shaped glass columns, 180 cm × 4 mm ID, were packed with either 3%

Abbreviations: GLC, gas–liquid chromatography; MS, mass spectrometry; RRT, relative retention time; TMS, trimethylsilyl; TMSO, trimethylsiloxyl. The following are the systematic names of bile alcohols referred to by trivial or abbreviated names: Δ^{24}-triol, 5β-cholest-24-ene-3α,7α,12α-triol; Δ^{25}-triol, 5β-cholest-25-ene-3α,7α,12α-triol; 23-tetrol, 5β-cholestane-3α,7α,12α,23ξ-tetrol; 24-tetrol, 5β-cholestane-3α,7α,12α,24ξ-tetrol; 25-tetrol, 5β-cholestane-3α,7α,12α,25-tetrol; 26-tetrol, 5β-cholestane-3α,7α,12α,26-tetrol; 22,25-pentol; 5β-cholestane-3α,7α,12α,22ξ,25-pentol; 23,25-pentol, 5β-cholestane-3α,7α,12α,23ξ,25-pentol; 24,25-pentol, 5β-cholestane-3α,7α,12α,24ξ,25-pentol; 25,26-pentol-5β-cholestane-3α,7α,12α,25,26-pentol; 24,26-pentol, 5β-cholestane-3α,7α,12α,24ξ,26-pentol.

QF-1 on 80/100 mesh Gas Chrom Q or 1% HI-EFF 8BP on 100/120 mesh Gas Chrom Q (Applied Science Labs.).

The GLC operating conditions were: column temperature 235°C; detector temperature 270°C; and carrier gas (N_2) flow, 40 ml/min.

Mass spectrometry (MS)

All mass spectra were obtained from a Varian Model MAT-111 electron impact, 90° magnetic sector GLC–mass spectrometer equipped with a mass spectrometer readout system (Model CSI-260, Columbia Scientific Industries, Inc.). The TMS derivatives of the bile alcohols were injected on 180 cm × 2 mm ID helical silanized glass columns with packings as described above. Helium at 15 ml/min was used as the GLC carrier gas.

The following operating temperatures were employed: injector 250°C, column 220–250°C, separator 270–280°C, inlet line (separator to ion source) 280–290°C. The ion current was 280 μA, accelerating voltage 820 V, and electron impact energy 80 eV.

TABLE 1. GLC of bile alcohols. Retention times of TMS ethers of bile alcohols relative to 5α-cholestane on 3% QF-1 and 1% HI-EFF 8BP

Compound	3% QF-1[a]	1% HI-EFF 8BP[b]
Cholesterol[c]	1.81	1.92
5β-Cholestane-3α-ol (Epicoprostanol)[c]	1.52	1.59
5β-Cholestane-3α,7α-diol[d]	1.69	1.14
5β-Cholestane-3α,12α-diol[d]	1.60	1.07
5β-Cholestane-3α,7α,26-triol[e]	3.35	2.28
5β-Cholestane-3α,7α,12α-triol[d]	1.64	0.70
5β-Cholest-24-ene-3α,7α,12α-triol[f]	1.80	0.91
5β-Cholest-25-ene-3α,7α,12α-triol[f]	1.81	0.89
5β-Cholestane-3α,7α,12α,23ξ-tetrol[g]	2.37	0.97
5β-Cholestane-3α,7α,12α,24ξ-tetrol[g]	2.65	1.11
5β-Cholestane-3α,7α,12α,25-tetrol[f]	2.98	1.25
5β-Cholestane-3α,7α,12α,26-tetrol[g,h]	3.24	1.56
5β-Cholestane-3α,7α,12α,22ξ,25-pentol[h]	3.90	1.67
5β-Cholestane-3α,7α,12α,23ξ,25-pentol[i]	3.90	1.58
5β-Cholestane-3α,7α,12α,24α,25-pentol[j]	4.22[k]	1.65[k]
5β-Cholestane-3α,7α,12α,24β,25-pentol[j]	4.35[k]	1.76[k]
5β-Cholestane-3α,7α,12α,25,26-pentol[h]	4.76	1.98
5β-Cholestane-3α,7α,12α,24ξ,26-pentol[h]	4.18	1.97

[a] Column 235°C; N = 40 ml/min; retention time of 5α-cholestane 2.75 min.
[b] Column 235°C; N = 40 ml/min; retention time of 5α-cholestane 7.08 min.
[c] Samples from Steraloids, Inc., Wilton, NH.
[d] Gift from Dr. I. Björkhem, Department of Clinical Chemistry, Karolinska Institute, Huddinge, Sweden.
[e] Synthesized (32).
[f] Synthesized (33).
[g] Isolated from bile and feces of patients with cerebrotendinous xanthomatosis (unpublished).
[h] Gift from Dr. T. Hoshita, Hiroshima School of Medicine, Hiroshima, Japan.
[i] Isolated from bile and feces of patients with cerebrotendinous xanthomatosis (12).
[j] Synthesized (12).
[k] The RRT for these two epimers are different with $P < 0.01$ on both columns (12).

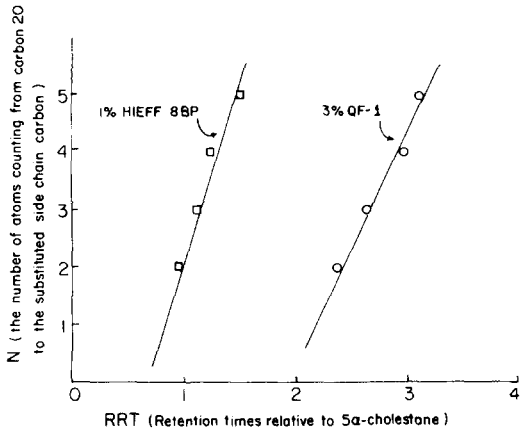

Fig. 1. Measured GLC retention times (RRT) relative to 5α-cholestane of the TMS 5β-cholestanetetrols on 3% QF-1 and 1% HI-EFF 8BP at 235°C and 40 ml/min N_2 plotted against N, the number of carbon atoms from carbon 20 to the TMSO-substituted side-chain carbon atom.

RESULTS AND DISCUSSION

Gas–liquid chromatography

The retention times of the TMS derivatives of the bile alcohols relative to 5α-cholestane are given in **Table 1.** The two unsaturated triols, namely 5β-cholest-24-ene-3α,7α,12α-triol and 5β-cholest-25-ene-3α,7α,12α-triol, could not be resolved on either column. Furthermore, 5β-cholestane-3α,7α,12α,22ξ, 25-pentol and 5β-cholestane-3α,7α,12α,23ξ,25-pentol were not resolved on 3% QF-1 columns, but were well separated on 1% HI-EFF 8BP. The latter column, however, showed the same retention time for 5β-cholestane-3α,7α,12α,22ξ,25-pentol and 5β-cholestane-3α,7α,12α,24α,25-pentol. 5β-Cholestane-3α,7α, 12α,25,26-pentol and 5β-cholestane-3α,7α,12α,24ξ, 26-pentol were very well separated on 3% QF-1, but appeared as a single peak on HI-EFF 8BP columns.

On both 3% QF-1 and 1% HI-EFF 8BP columns the relative retention times (RRT) of the 5β-cholestanetetrols varied linearly with N, the number of carbon atoms counting from carbon 20 to the carbon bearing the trimethylsiloxyl (TMSO) group (e.g., for the TMS ether of 5β-cholestane-3α,7α,12α,23ξ-tetrol, N = 2; for the TMS ether of 5β-cholestane-3α,7α, 12α,24ξ-tetrol, N = 3, etc.) (**Fig. 1**). However, no linearity was observed when the RRT values for the various pentols studied were plotted against the sum

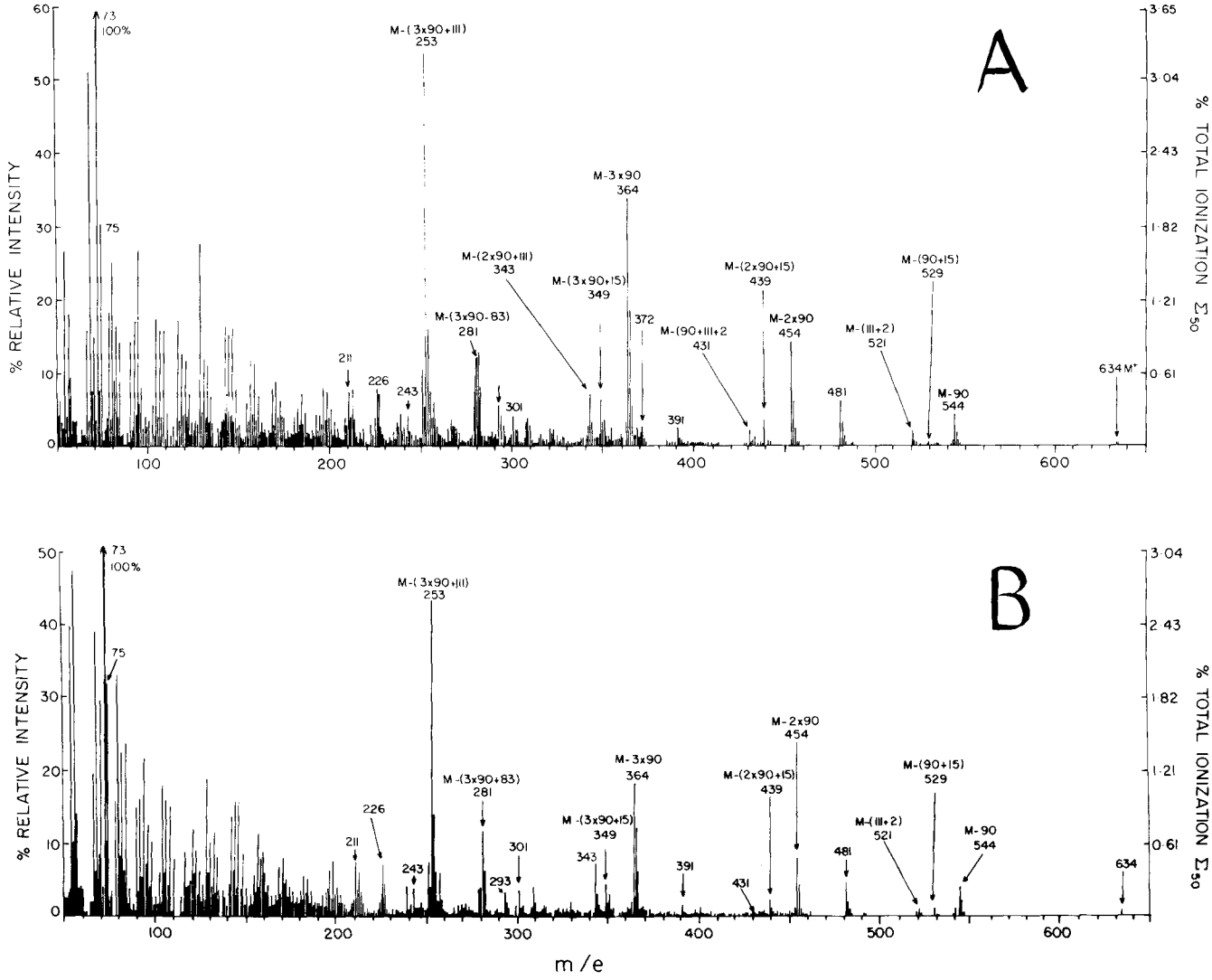

Fig. 2. *A*. Mass spectrum of TMS 5β-cholest-24-ene-3α,7α,12α-triol. *B*. Mass spectrum of TMS 5β-cholest-25-ene-3α,7α,12α-triol.

of the number of carbon atoms counting from carbon 22 to the carbons bearing the two TMSO groups.

As seen in Table 1, using 3% QF-1 columns, the effect of the addition of a TMSO substituent in the side chain on the RRT was much greater than that of a TMSO substituent added to the nucleus. Thus, the RRT of the TMS ether of 5β-cholestane-3α,7α,12α-triol (RRT 1.64) was almost identical with that of 5β-cholestane-3α,7α-diol (RRT 1.69) while the RRT of the TMS ether of the 3α,7α,26-triol (RRT 3.35) was about 98% greater than that of the corresponding 3α,7α-diol. On the other hand, elution of the bile alcohols from the 1% HI-EFF 8BP column was strongly influenced by the nuclear TMSO substituents. The TMS ethers of 5β-cholestan-3α-ol (RRT 1.59), 5β-cholestane-3α,7α-diol (RRT 1.14), and 5β-cholestane-3α,7α,12α-triol (RRT 0.70) showed a linear decrease of RRT values with the addition of nuclear TMSO groups. In fact the elution pattern was similar to that of the corresponding TMS ethers of the methyl esters of the mono-, di-, and trihydroxy bile acids when chromatographed under the same conditions (3α-hydroxy-5β-cholanoic acid, RRT 4.03; 3α,7α-dihydroxy-5β-cholanoic acid, RRT 2.86; and 3α,7α,12α-trihydroxy-5β-cholanoic acid, RRT 1.79).

Mass spectrometry

5β-Cholestane-3α,7α,12α-triol, 5β-cholest-24-ene-3α, 7α,12α-triol and 5β-cholest-25-ene-3α,7α,12α-triol. In **Fig. 2,** *A* and *B* show the mass spectra of the TMS ethers of 5β-cholest-24-ene-3α,7α,12α-triol and 5β-cholest-25-ene-3α,7α,12α-triol. Both exhibited a base peak at *m/e* 73, and major peaks at *m/e* 634, (M^+);

544, (M − 90); 529, [M − (90 + 15)]; 521, [M − (111 + 2)]; 454, [M − (2 × 90)]; 439, [M − (2 + 90 + 15)]; 364, [M − (3 × 90)]; 349, [M − (3 × 90 + 15)]; 343, [M − (2 × 90 + 111)]; 281, [M − (3 × 90 + 83)]; and 253, [M − (3 × 90 + 111)]. The relative intensities of the major fragments in the mass spectra of the above unsaturated triols appeared to be similar to those of the corresponding peaks in the saturated triol except for the base peak (found at *m/e* 253 for the saturated triol (16), and at *m/e* 73 for the unsaturated ones).

However, a careful examination of the spectra of the three triols in the region *m/e* 277 to *m/e* 285 (**Fig. 3**) revealed significant differences. In the saturated and the Δ^{25}-unsaturated triols the peak at *m/e* 281 was the dominant one while the intensity of the peaks at *m/e* 280 and 282 was less than 50% of *m/e* 281. The Δ^{24}-triol, however, presented an entirely different pattern, one in which the *m/e* 280, 281, and 282 peaks formed a triplet of approximately equal intensities. The fragment *m/e* 281 is formed by the cleavage of the side chain at carbons 20–22 plus the loss of all three trimethylsilanol groups (17, 18). The *m/e* 282 peak observed in the spectrum of the Δ^{24}-triol probably involved hydrogen transfer to the charged fragment. A suggested mechanism is shown in **Fig. 4.** It requires the loss of the TMSO function at C-12 and a hydrogen at C-11, charge localization in this region, and the subsequent transfer of a C-23 hydrogen to the nucleus. Inspection of a molecular model of the Δ^{24}-triol showed that, with free rotation of the side chain about the C-17 to C-20 bond axis, carbon 23 can approach to within about 1.7 Å of carbon 12. This is only 10% larger than the carbon–carbon tetrahedral bond distance of 1.5 Å. However, the fragment *m/e* 281 is very often a significant background peak arising from silicone phase column bleed, but the background at *m/e* 280 and 282 is usually quite small. Therefore, the presence of the

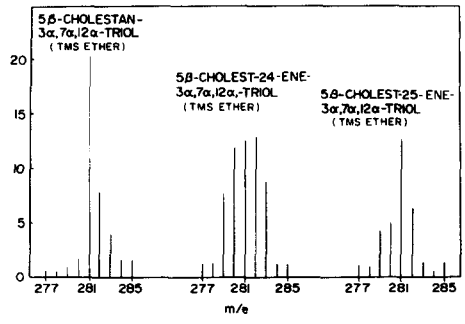

Fig. 3. Mass spectra of TMS 5β-cholestane-3α,7α,12α-triol, TMS 5β-cholest-24-ene-3α,7α,12α-triol, and TMS 5β-cholest-25-ene-3α,7α12α-triol in the region between *m/e* 277 and 285.

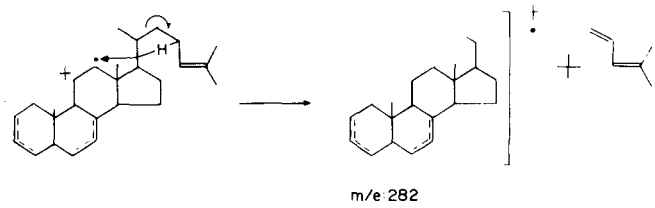

Fig. 4. Suggested origin of the *m/e* 282 peak in the spectrum of 5β-cholest-24-ene-3α,7α,12α-triol.

m/e 280 and 282 peaks at 10–15% relative intensity should serve as a positive indication of the Δ^{24}-triol.

5β-Cholestanetetrols and 5β-cholestanepentols (Tables 2 and 3). The mass spectra of the TMS ethers of these compounds contained many diagnostic peaks characteristic of the individual side-chain hydroxylation sites which were less prominent in the spectra of the underivatized samples (11). These side-chain fragmentation patterns first described for the TMS

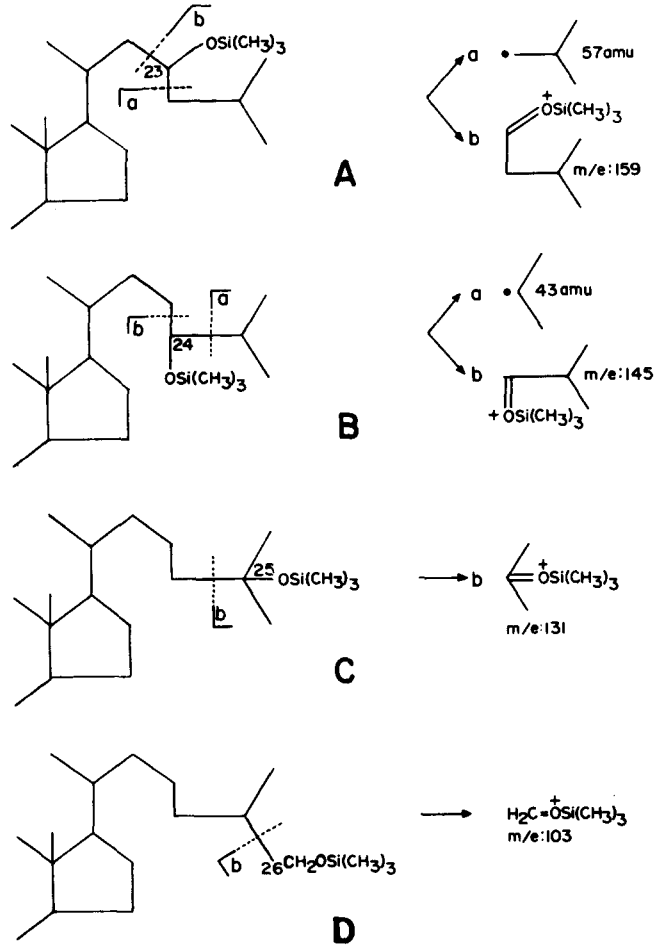

Fig. 5. Major side-chain fragmentation processes of the TMS 5β-cholestanetetrols. *A*, 5β-Cholestane-3α,7α,12α,23-tetrol TMS; *B*, 5β-cholestane-3α,7α,12α,24-tetrol TMS; *C*, 5β-cholestane-3α,7α,12α,25-tetrol TMS; and *D*, 5β-cholestane-3α,7α,12α,26-tetrol TMS.

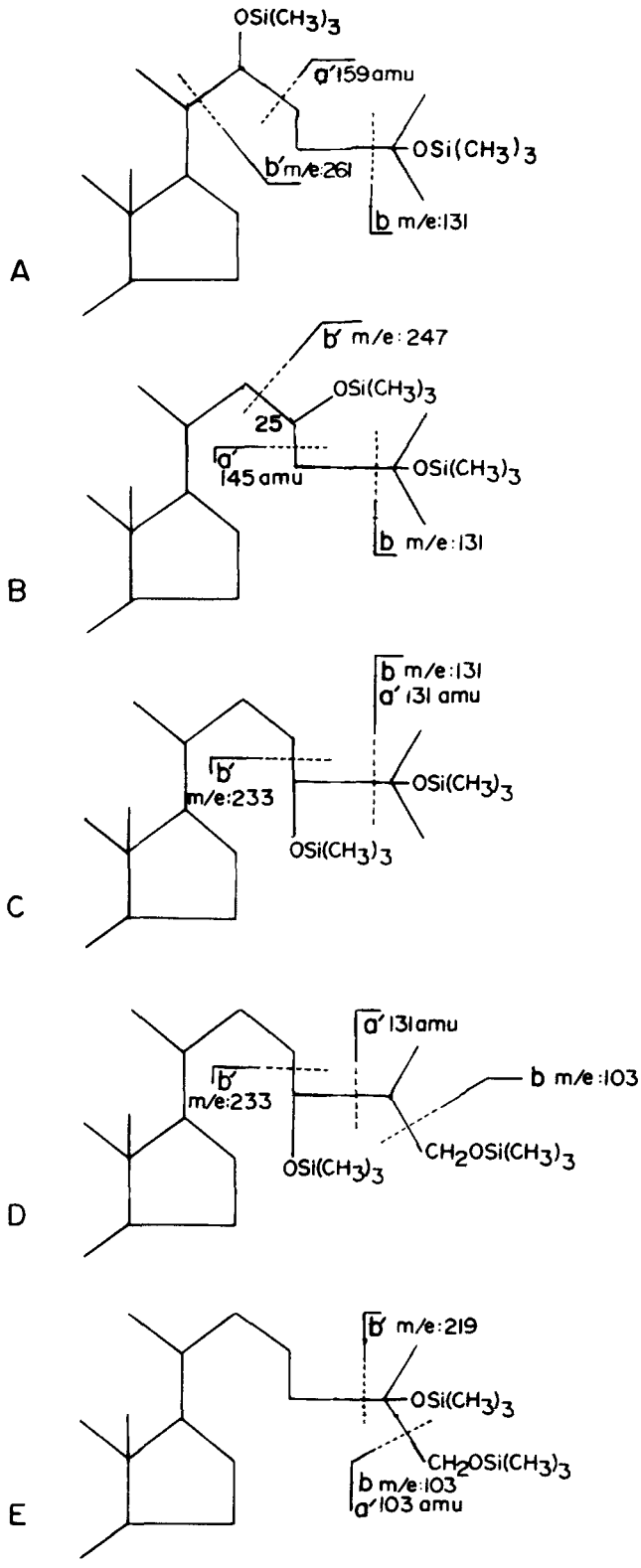

Fig. 6. Major side-chain fragmentation processes of the TMS 5β-cholestanepentols. *A*, 5β-cholestane-3α,7α,12α,22,25-pentol TMS; *B*, 5β-cholestane-3α,7α,12α,23,25-pentol TMS; *C*, 5β-cholestane-3α,7α,12α,24,25-pentol TMS; *D*, 5β-cholestane-3α,7α,12α,24,26-pentol TMS; and *E*, 5β,cholestane-3α,7α,12α,25,26-pentol TMS.

ethers of the cholestanetetrols by Cronholm and Johansson (8) and later observed for the TMS ethers of the cholestanepentols (11, 12, 19) suggest that each side-chain TMSO substituent can give rise to two separate fragmentation effects. Each of these derives from cleavage of the bonds connected to a TMSO-substituted carbon and each in turn gives rise to a distinct series of fragmentation peaks.

In what follows, cleavage *a* represents the breaking of the bond between the TMSO-substituted carbon and its neighboring carbon atom that is closer to the terminal end of the side chain. Conversely, cleavage *b* refers to the rupture of the bond between the TMSO-substituted carbon and the carbon atom nearer to the nucleus. Since there are two TMSO groups in the side chain of the cholestanepentols studied by us, we will designate the cleavages associated with the TMSO-substituted carbon closest to the nucleus as *a'* and *b'* and the cleavages associated with the substituted carbon closest to the end of the side chain as *a* and *b*. Cleavage *a* (or *a'*) results in the loss of a *neutral* fragment consisting of the terminal portion of the side chain beginning with the carbon atom α to the TMSO-substituted carbon. Cleavage at *b* (or *b'*), on the other hand, produces a *charged* fragment which consists of the TMSO-substituted carbon plus all of the attached terminal portion of the side chain.

Cleavage at *a* will usually give rise to a series of mass peaks since polytrimethylsiloxyl compounds usually lose successive molecules of trimethylsilanol, $HOSi(CH_3)_3$, 90 amu (20, 21). The series will start with a mass peak *m/e* equal to M (the molecular weight) minus the mass of the lost neutral fragment, and will show peaks due to successive losses of 90 mass units. A TMS ether of cholestanetetrol can exhibit a maximum of five of these peaks [e.g., 5β-cholestane-3α,7α,12α,23ξ-tetrol (**Fig. 5*A***) exhibits the series *m/e* 667 (M − 57), 577 (M − 57 − 90), 487, 397 and 307 (8)], while a TMS ether of a cholestanepentol can yield a series of six peaks.

In the TMS ethers of cholestanepentols, cleavage *a'* will result in the loss of a considerably heavier neutral fragment containing a TMSO-substituted carbon and will give rise to a series of five peaks, 90 mass units apart [e.g., the series 667 (M − 145), 577, 487, 397, and 307 in the mass spectrum of 5β-cholestane-3α,7α,12α,23ξ,25-pentol (11) (**Fig. 6*B***)]. Cleavage *b*, on the other hand, will usually give rise to only one peak which consists of the charged terminal side-chain fragment and is the origin of the intense peak at *m/e* 145 in 5β-cholestane-3α,7α,12α,24-tetrol (8) (**Table 2;** Fig. 5*B*). Cleavage *b'* can, however, yield two peaks; the heavier one will consist

TABLE 2. % Relative intensities (% int) and % total ionization: Σ_{50} (% ion) for major diagnostic fragment peaks of TMS ethers of 5β-cholestanetetrols

Fragment Ion	m/e	3α,7α,12α,23-Tetrol[a]		3α,7α,12α,24-Tetrol[a]		3α,7α,12α,25-Tetrol[a,b]		3α,7α,12α,26-Tetrol	
		% Int	% Ion	% Int	% Ion	% Int	% Ion	% Int	% Ion
M^+	724			0.4	0.02	0.1	0.01	0.4	0.02
M − 43[c]	681			2.1	0.09				
M − 57	667	2.2	1.9						
M − 90	634	0.7	0.07	2.2	0.09	0.5	0.04	3.2	0.19
M − (90 + 43)[c]	591			2.3	0.10				
M − (90 + 57)[c]	577	1.1	0.10						
M − (2 × 90)	544	6.3	0.55	13	0.60	6.2	0.52	52	3.1
M − (2 × 90 + 43)[c]	501			8.2	0.37				
M − (2 × 90 + 57)[c]	487	1.9	0.16						
M − (3 × 90)	454	8.2	0.71	20	0.88	14	1.2	56	3.3
M − (3 × 90 + 43)	411			18	0.79				
M − (3 × 90 + 57)	397	3.1	0.27						
M − (4 × 90)	364	12	1.0	10	0.44	14	1.2	1.7	0.10
M − (2 × 90 + 201SC[d])	343	11	0.95	24	1.1	10	0.84	37	2.2
M − (4 × 90 + 43)	321			47	2.1				
M − (4 × 90 + 57)	307	9.2	0.80						
M − (3 × 90 + 201SC[d])	253[e]	33	2.9	55	2.5	48	4.1	89	5.2
Charged terminal side-chain fragment[f]	159	100	8.7						
Charged terminal side-chain fragment[f]	145			64	2.9				
Charged terminal side-chain fragment[f]	131					100	8.4		
Charged terminal side-chain fragment[f]	103							14	0.83
$Si(CH_3)_3$	73	52	4.5	100	4.5	70	5.9	100	5.9

[a] Reference 8.
[b] Reference 11.
[c] Process *a* (see text).
[d] Entire side chain: 201 amu.
[e] Tri-unsaturated steroid nucleus.
[f] Process *b*: charged terminal side-chain fragment (see text).

of a charged side-chain fragment that has retained both side-chain trimethylsiloxyl substituents. This will give rise to the lighter fragment by the loss of one molecule of trimethylsilanol (90 amu). Thus, in the mass spectrum of the TMS ether of 5β-cholestane-3α,7α,12α,24ξ,25-pentol (12) (Fig. 6*C*), these processes account for the peaks at *m/e* 247 and 157 (247 − 90).

Occasionally, cleavage at *b* will result in a fragmentation in which charge is retained on the heavier fragment containing the nucleus. This will lead to a series of mass peaks differing by 90 amu, as in cleavage *a*. Such peaks are usually of small relative intensity and are most evident in the spectra of C-26 TMSO-substituted compounds (**Tables 2** and **3**).

Cleavages *a′* and *b′* have been observed in the mass spectra of the TMS ethers of cholestanepentols (11, 12, 19) and cleavage *a′* has been seen with the TMS ether of 5α-pregnane-3α,20α,21-triol (22). In addition, cleavage *b* has been observed in the mass spectrum of 25-hydroxyergocalciferol (23), cleavages *a′* and *b′* have been seen in silylated ecdysone (5β-cholest-7-ene-2β,3β,14α,22α,25-pentol-6-one) (24), cleavages *a*, *b*, *a′*, and *b′* have been seen in 20α,22(*RS*)-dihydroxycholesterol (25) while cleavage *a* was detected in 25,26-dihydroxycholecalciferol (26). Cleavage *a* in a cholestanepentol with a 26-TMSO substituent is not possible, while a 25-TMSO substituent would induce the loss of a C-26 or C-27 methyl group (15 amu). However, the loss of a methyl group is so common in sterols that it cannot be specifically ascribed to the effect of the 25-TMSO group.

Mass spectra of TMS ethers of 5β-cholestanetetrols (Table 2, Fig. 5). The mass spectra of the TMS ethers of several 5β-cholestanetetrols, namely 5β-cholestane-3α,7α,12α,23ξ-tetrol; 5β-cholestane-3α,7α,12α,24ξ-tetrol, 5β-cholestane-3α,7α,12α,25-tetrol, and 5β-cholestane-3α,7α,12α,26-tetrol, were first described by Cronholm and Johansson (8). Mass spectra of a series of 5α-cholestanetetrols have recently been described by Ali and Elliot (27) and are very similar to those obtained from the 5β-series. Except perhaps for the TMS ether of 5β-cholestane-3α,7α,12α,26-tetrol, side-chain fragmentations, as described above, provide ample diagnostic peaks. Important peaks in the mass spectra of the 5β-cholestanetetrols are summarized in Table 2 and their side-chain fragmentations are indicated diagrammatically in Fig. 5.

In the mass spectrum of 5β-cholestane-3α,7α,12α,23ξ-tetrol, cleavage *a* (Fig. 5*A*) led to the loss of a

TABLE 3. % Relative intensity (% int) and % total ionization: Σ_{50} (% ion) for major diagnostic peaks of TMS ethers of 5β-cholestanepentols

Fragment Ion[a]	m/e	3α,7α,12α,22α, 25-Pentol[b]		3α,7α,12α,23ξ, 25-Pentol[c]		3α,7α,12α,24ξ, 25-Pentol[d,e]		3α,7α,12α, 24ξ,26- Pentol[f]		3α,7α,12α, 25,26- Pentol[g,h]	
		% Int	% Ion	% Int	% Ion	% Int	% Ion	% Int	% Ion	% Int	% Ion
M − 103	709									10	0.72
M − 131	681					0.20	0.06	3.7	0.23		
M − 145	667			0.57	0.16						
M − 159	653	0.23	0.06								
M − (90 + 103)	619									6.2	0.42
M − (90 + 131)	591					0.30	0.09	4.3	0.26		
M − (90 + 145)	577			0.27	0.07						
M − (90 + 159)	563	0.28	0.08								
M − (2 × 90 + 103)	529									31	2.2
M − (2 × 90 + 131)	501					0.96	0.28	20	1.2		
M − (2 × 90 + 145)	487			0.53	0.14						
M − (2 × 90 + 159)	473	0.35	0.11								
M − (3 × 90 + 103)	439									31	2.1
M − (3 × 90 + 131)	411					2.0	0.58	37	2.3		
M − (3 × 90 + 145)	397			1.0	0.28						
M − (3 × 90 + 159)	383	1.0	0.32								
M − (4 × 90 + 103)	349									46	3.2
M − (4 × 90 + 131)	321					4.8	1.4	55	3.4		
M − (4 × 90 + 145)	307			3.3	0.91						
M − (4 × 90 + 159)	293	1.6	0.49								
Charged side-chain fragment[i]	261	2.2	0.68								
Charged side-chain fragment[i]	247			0.20	0.05						
Charged side-chain fragment[i]	233					0.53	0.15	52	3.2		
Charged side-chain fragment[i]	219									33	2.3
Charged side-chain fragment[j]	171	100	30								
Charged side-chain fragment[j]	157			5.3	1.4						
Charged side-chain fragment[j]	143					3.8	1.1	28	1.7		
Charged terminal side-chain fragment[k]	131	9.4	2.8	100	27	100	28.8				
Charged side-chain fragment[j]	129									19	1.3
Charged terminal side-chain fragment[k]	103							77	4.7	9.6	0.66

[a] Process *a'* (see text).
[b] References 21, 28.
[c] References 11, 12.
[d] The spectra of the 24α and 24β epimers are the same.
[e] Reference 12.
[f] Base peak *m/e* 73; 6.1% total ionization.
[g] Base peak *m/e* 73; 6.9% total ionization.
[h] Reference 28.
[i] Process *b'* (see text).
[j] Process *b'*; fragment minus trimethylsilanol (90 amu) (see text).
[k] Process *b* (see text).

neutral fragment of 57 amu composed of carbons 24 to 27, $\cdot CH_2CH(CH_3)_2$, and gave rise to a fragmentation series at *m/e* 667, (M − 57); 577, [M − (90 + 57)]; 487, [M − (2 × 90 + 57)]; 397, [M − (3 × 90 + 57)]; and 307, [M − (4 × 90 + 57)]. Mechanism *b* (Fig. 5*A*) caused rupture of the bond between carbons 22 and 23 with the formation of the base peak $[(CH_3)_3 - \dot{Si}O{=}CHCH_2CH(CH_3)_2]$, at *m/e* 159. Cleavage *a* in the 5β-cholestane-3α,7α,12α,24ξ-tetrol (Fig. 5*B*) resulted in the loss of the 43 amu isopropyl group from the side chain and yielded a series at *m/e*: 681, (M − 43); 591, [M − (90 + 43)]; 501, [M − (2 × 90 + 43)]; 411, [M − (3 × 90 + 43)]; and 321, [M − (4 × 90 + 43)]. The charged side-chain fragment $[(CH_3)_3Si\dot{O}{=}CHCH(CH_3)_2]$ that resulted from cleavage between carbons 23 and 24 (Fig. 5*B*) was found at *m/e* 145, as Cronholm and Johansson reported for this compound (8). In the present experiments *m/e* 145 was a major peak (Table 2), but the most intense fragment occurred at *m/e* 73 $[\dot{Si}(CH_3)_3]$. This difference may be ascribed to different operating conditions or to column bleed.

Cleavage *a* in 5β-cholestane-3α,7α,12α,25-tetrol (Fig. 5*C*) would lead to a loss of CH_3 (15 amu), but this is not distinguishable from the loss of methyl groups that occurs during the mass spectrometry of most sterols. Cleavage *b* (Fig. 5*C*) gave rise to the base peak $[(CH_3)_3Si\dot{O}{=}C(CH_3)_2]$ at *m/e* 131. 5β-Cholestane-3α,7α,12α,26-tetrol yields only a low-intensity fragment from cleavage *b* at *m/e* 103

$[(CH_2{=}\dot{O}Si(CH_3)_3]$ (Fig. 5D), which is not of major importance for identification of this tetrol.

Two low-intensity side-chain cleavage series were visible in the spectrum of this compound. The first of these was seen at *m/e* 503 (1%), 413 (2%), and 323 (1%), M − (90 + 131), M − (2 × 90 + 131), etc., and could have arisen from carbon 24–25 cleavage (loss of C-25 to C-27) while the second consisted of small peaks appearing at *m/e* 399 (2%) and 309 (2%), M − (2 × 90 + 145) and M − (3 × 90 + 145), possibly due to C-23,24 cleavage (loss of C-24 to C-27). These kinds of fragments were probably generated either by the loss of the C-26 TMSO group or by the loss of carbon 26 itself with charge retention on the remaining side chain. Following this, a two-step electron transfer could then serve both to move the charge along the side chain toward the nucleus and to cleave the more terminal portion.

Mass spectra of the TMS ethers of 5β-cholestane-3α,7α,12α,22ξ,25-pentol, 5β-cholestane-3α,7α,12α,23ξ,25-pentol, 5β-cholestane-3α,7α,12α,24ξ,25-pentol, 5β-cholestane-3α,7α,12α,25,26-pentol (Table 3; Figs. 6 and 7)

The mass spectra of the above 5β-cholestanepentols exhibit similar patterns of side-chain fragmentations as described above for the cholestanetetrols. These mechanisms are summarized in Figure 6 and the observed mass peaks due to side-chain fragmentations are listed in Table 3. The spectra of 5β-cholestane-3α,7α,12α,23ξ,25-pentol (11, 12), -3α,7α,12α,24ξ,25-pentol (12), and -3α,7α12α,22ξ,25-pentol (19, 28) have been published previously. The spectrum of the 5β-cholestane-3α,7α,12α,25,26-pentol (28, 29) has been described, but a complete spectrum was not given.

The base peak of 5β-cholestane-3α,7α,12α.22ξ,25-pentol detected at *m/e* 171 (261 − 90) (Table 3) arises from the *m/e* 261 fragment $[(CH_3)_3Si\dot{O}{=}CH(CH_2)_2C(CH_3)_2OSi(CH_3)_3]$ formed by C-20,22 scission (*b′*) (Fig. 6*A*) which loses one molecule of trimethylsilanol. Together, the *m/e* 261 and 171 fragments carried almost 31% of the total ion current (Table 3) while the tertiary charged terminal side-chain fragment (*m/e* 131) carried only 2.8%. Also visible in the spectrum of this compound was C-22,23 scission, yielding the series at *m/e* 563, M − (90 + 159); 473, 383, and 293 (Table 3). The mass spectrum of the TMS derivative of cholest-5-ene-3β,22-diol (22-hydroxycholesterol; Ikapharm, Ltd., Ramat, Israel) obtained on the same instrument showed very similar behavior (not illustrated): The base peak was at *m/e* 173 $[(CH_3)_3Si\dot{O}{=}CH(CH_2)_2CH(CH_3)_2]$ (C-20,22 scission). The *m/e* 83 (173 − 90) peak had a relative intensity of 66% and these two peaks, together, carried 58% of the total ion current. The expected series due to C-22,23 scission at *m/e* 475, (M − 71), 385, M − (90 + 71) and 295, M − (2 × 90 + 71) was also found in the spectrum of 22-hydroxycholesterol.

In contrast to the behavior of the 5β-cholestane-3α,7α,12α,22ξ,25-pentol, the base peak in the spectrum of 5β-cholestane-3α,7α,12α,23ξ,25-pentol (11, 28) was at *m/e* 131 and carried 27% of the total ion current (Table 3) while the fragment seen at *m/e* 247 was very small and the peak at *m/e* 157 (247 − 90) had a relative intensity of only 5.3%. The side-chain cleavage series (C-23,24 cleavage) (a′, Fig. 6*B*) was detectable and served to identify carbon 23 as the site of a trimethylsilanol substituent. These fragments appeared at *m/e* 667, (M − 145), 577, M − (90 + 145), 487, 397, and 307 (Table 3).

The spectra of 5β-cholestane-3α,7α,12α,24α,25-pentol and 5β-cholestane-3α,7α,12α,24β,25-pentol were identical (12) and were similar to the mass spectrum of the -3α,7α,12α,23ξ,25-pentol except for the series derived from C-24,25 cleavage (Fig. 6*C*), which appeared at *m/e* 681, (M − 131), 591, 501, 411, and 321, which differs by 14 amu from the corresponding series from 5β-cholestane-3α,7α,12α,23ξ,25-pentol (Table 3). The base peak at *m/e* 131 carried almost 29% of the total ion current (Table 3), while the more massive charged side-chain fragments at *m/e* 233 (*b′*) and *m/e* 143 (233 − 90) (Fig. 6*C*) carried 0.15% and 1.1%, respectively (Table 3).

Without the C-22, C-23, or C-25 TMSO substituent to direct side-chain fragmentation, the spectrum of 5β-cholestane-3α,7α,12α,24ξ,26-pentol (27-deoxyscymnol) (**Fig. 7*A***) showed no overwhelmingly large fragment ions derived from the side chain and the base peak appeared at *m/e* 73 $[^+Si(CH_3)_3]$. The peak with the highest intensity (77%, Table 3), due to side-chain fragmentation arose from cleavage *b* (Fig. 6*D*) and was detected at *m/e* 103 $[(CH_3)_3SiOCH_2)]^+$, while the *m/e* 233 $[(CH_3)_3Si\dot{O}{=}CHCH(CH_3)CH_2OSi(CH_3)_3]$ and 143 (233 − 90) peaks had relative intensities of 52% and 28% respectively (Table 3). Since one or two fragments alone did not carry an overwhelming portion of the total ion current, the side-chain fragmentation series, due to loss of 131 amu, *m/e* 681, 591, 501, and 411 and 321 became quite prominent (Table 3). An additional weak cleavage series could also be detected at *m/e* 474 (6%), 384 (2.5%), and 294 (9%) [M − 248, M − (90 + 248) and M − (2 × 90 + 248)]. It is probably due to C-22,23 scission (loss of 247 amu) plus the loss of an additional hydrogen atom with charge retention on the more massive fragment. This series might possibly be formed in a manner similar to the series seen in the mass spectrum of 5β-cholestane-3α,7α,12α,26-tetrol at *m/e* 503, 413, and 313.

The mass spectrum of 5β-cholestane-3α,7α,12α,25,

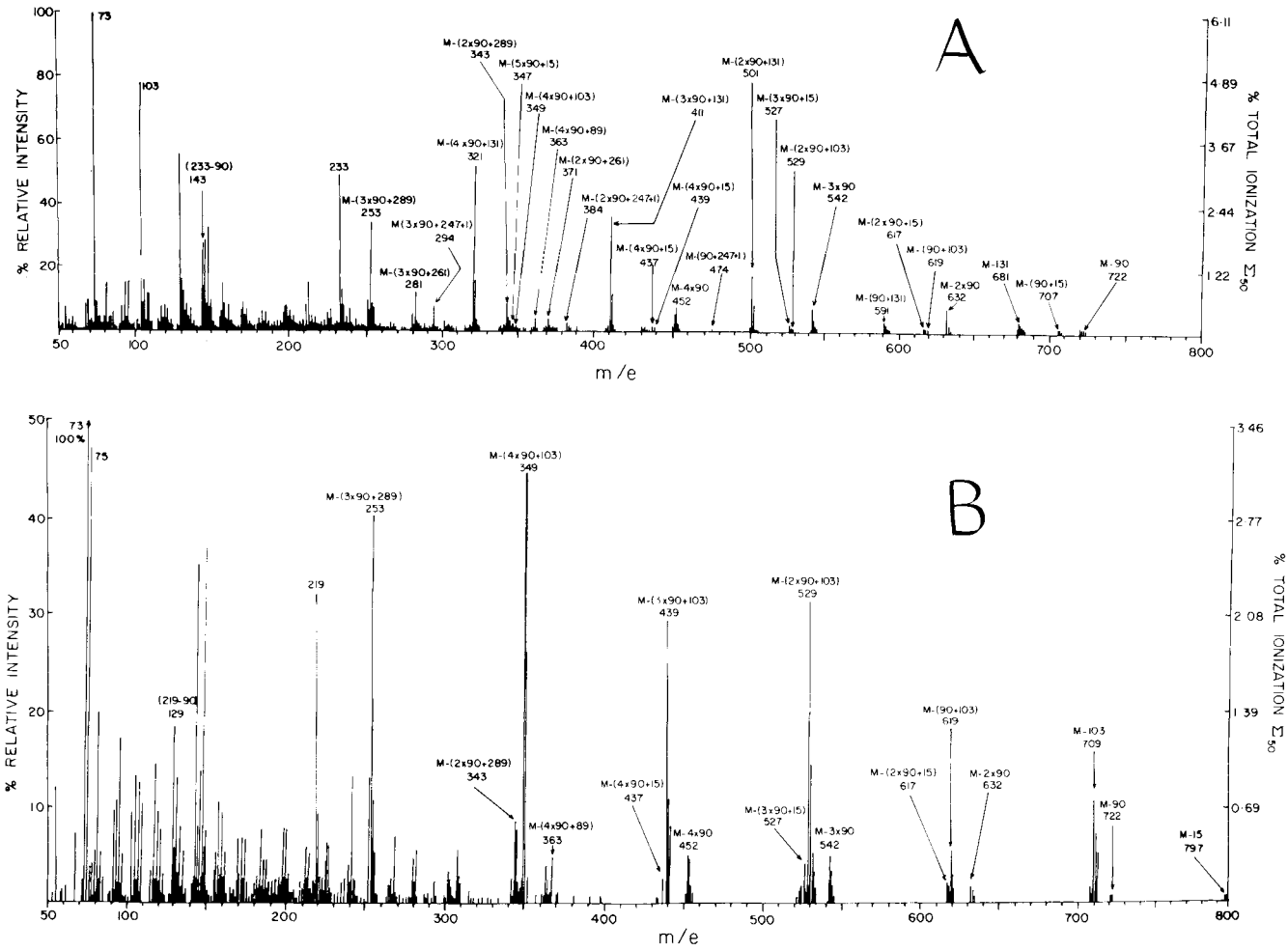

Fig. 7. *A*. Mass spectrum of TMS 5β-cholestane-3α,7α,12α,24ξ,26-pentol. *B*. Mass spectrum of TMS 5β-cholestane-3α,7α,12α,25,26-pentol.

26-pentol (Fig. 7*B*) may easily be distinguished from that of the -3α,7α,12α,24ξ,26-pentol (Fig. 7*A*) by the increased prominence in the former of the side-chain cleavage series seen at *m/e* 709, 619, 529, and 439 (loss of 103 amu, Fig. 6*E*) (Table 3). The charged terminal side-chain fragment *m/e* 103 (*b*) was quite small. In contrast, the more massive charged side-chain fragment (*b'*) found at *m/e* 219 [$(CH_3)_3SiO{=}C(CH_3)OSi(CH_3)_3$] (33% relative intensity) was more prominent as was the analogous *m/e* 233 peak in the mass spectrum of 5β-cholestane-3α,7α,12α,24ξ,26-pentol.

Stability of side chain fragments. Although each of the side-chain TMSO substituents caused a very predictable fragmentation pattern, the magnitude of the effect varied considerably. Of the tetrols and pentols studied, the C-22 TMSO substituent produced the most intense charged side-chain fragments. In the spectrum of the C-22,25-TMSO cholestanepentol (Table 3), the charged side-chain fragments produced by C-20,22 bond cleavage found at *m/e* 261 and 171 accounted for more than 30% of the total ion current. The corresponding fragments in the spectrum of TMS 22-hydroxy cholesterol seen at *m/e* 173 and 83 carried more than 50% of the ion current. A trimethylsiloxyl group at carbon 23 was less influential than one at C-22 in directing fragmentation, but it was stronger than one at C-24. This can be inferred by comparing the spectra of the TMS C-23 and C-24 tetrols (Table 2). The base peak of the former appeared at *m/e* 159 while the base peak of the latter tetrol was found at *m/e* 73 and the charged *m/e* 145 side chain had a relative intensity of only 64%. A TMSO substituent at carbon 25 had an effect whose magnitude was between that of the TMSO-substituted carbons 22 and 23. The base peak of the TMS 23,25-pentol appeared at *m/e* 131 (Table 3), a fragmentation directed by carbon 25, and not at *m/e* 247 or 157

which would have occurred if the TMSO substituent at C-23 were more influential.

The high intensity of the *m/e* 131 charged side-chain fragment that arises from C-24,25 scission was expected, since it consists of an ion containing the very stable tertiary carbon 25. A rationale for the bond cleavage probabilities and resulting relative fragmentation-directing abilities of carbons 22, 23, and 24 may reside in the relative stabilities of the neutral free radical moieties (30) remaining after cleavage of the charged side-chain fragment.

Rupture of the C-20,22 bond would result in the stable secondary C-20 radical (18). Cleavage of the C-22,23 bond would result in the less stable C-22 radical, while C-23,24 cleavage would produce a radical with the least stable configuration in which the unpaired electron is farthest from the stabilizing effects of carbon 20. In every case, the resulting stable charged side-chain fragment is an even-electron ion (30).

A TMSO substituent on the terminal C-26 methyl carbon had almost no ability to direct the production of a charged side-chain fragment, probably because loss of carbon 26 and its TMSO substituent leads to charge retention on carbon 25 with the formation of a more stable tertiary carbonium ion rather than a charged secondary carbon 26 fragment (31). This would account for the unusually prominent M − 103 peak at *m/e* 709 in the spectrum of the TMS 25,26-pentol which had a relative intensity of 10% (Table 3). It may also be the reason for the somewhat unexpected appearance of the weak M − 103 series at *m/e* 619, 529, 439, and 349 in the spectrum of the TMS 24,26-cholestanepentol and the varied side-chain fragmentations in the TMS 26-cholestanetetrol.

Conclusion

There are sufficient regularities both in the GLC retention times and in the mass spectral fragmentation patterns of the TMS derivatives of the tetra- and pentahydroxy bile alcohols to permit their positive identification, even without reference compounds for comparison. The observed regularities in the mass spectra are due largely to TMSO substituents in the side chain. A possible explanation of the effect of the C-22, 23, 24, and 25 TMSO substituents may be the relative stabilities of the neutral free radical that remains after side-chain cleavage. Confirmation of many of the suggested fragmentation mechanisms will, however, have to await stable isotope labeling studies and high-resolution mass measurements.

The observations dealing with the fragmentation patterns in the mass spectra of the 5β-cholestane-triols, -tetrols, and -pentols, and 5β-cholest-ene-triols may be summarized as follows.

1. A TMSO substituent in the side chain will usually produce intense, predictable charged side-chain fragments.
2. The most intense fragments tend to be those from the side chain formed by cleavage of the carbon–carbon bond α to the TMSO-substituted carbon on the side toward the steroid nucleus.
3. Cleavage of the bond α to the TMSO-substituted carbon to the terminal portion of the side chain leads to a series of peaks carrying the nucleus.
4. A TMSO substituent at C-22 is most effective at directing side-chain scission, probably because of the formation of the stable secondary free radical at carbon 20.
5. A TMSO group at C-25 is almost as effective as one at C-22 since it can form a tertiary carbonium ion at C-25. A TMSO group at C-23 is less effective, followed by one at C-24 and then at C-26.
6. A side chain with a TMSO substituent at C-26 will often result in the loss of carbon 26 with the charge being retained on the side chain, probably at the tertiary carbon 25. This, in turn, leads to the production of a variety of weak side-chain fragments.
7. A TMSO substituent at carbon 12 appears to affect the side-chain fragmentation of cholestenetriols with an unsubstituted, unsaturated side chain.

This work was supported by U.S. Public Health Service grants AM-19696, AM-18707, HL-17818, AM-05222, and HL-10894.

Manuscript received 14 March 1977 and in revised form 28 September 1977; accepted 10 April 1978.

REFERENCES

1. Haslewood, G. A. D. 1967. Bile salt evolution. *J. Lipid Res.* **8:** 535–550.
2. Haslewood, G. A. D. 1967. Bile Salts. Methuen & Co., Lt., London. 72–81.
3. Hoshita, T., and T. Kazuno. 1968. Chemistry and metabolism of bile alcohols and higher bile acids. *In* Advances in Lipid Research, Vol. 6. R. Paoletti and D. Kritchevsky, editors. Academic Press, New York. 207–254.
4. Matschiner, J. T. 1971. Naturally occurring bile acids and alcohols and their origins. *In* The Bile Acids. Vol. 1. P. P. Nair and D. Kritchevsky, editors. Plenum Press, New York. 35–41.
5. Mosbach, E. H. 1972. Hepatic synthesis of bile acids. *Arch. Int. Med.* **130:** 478–487.
6. Danielsson, H. 1973. Mechanisms of bile acid synthesis. *In* The Bile Acids, Vol. 2. P. P. Nair and D. Kritchevsky, editors. Plenum Press, New York. 1–32.
7. Björkhem, I., and H. Danielsson. 1974. Hydroxylations in biosynthesis and metabolism of bile acids. *Mol. Cell. Biochem.* **4:** 79–95.
8. Cronholm, T., and G. Johansson. 1970. Oxidation of

5β-cholestane-3α,7α,12α-triol by rat liver microsomes. *Eur. J. Biochem.* **16:** 373–381.
9. Björkhem, I., and J. Gustafsson. 1973. ω-Hydroxylation of steroid side chain in biosynthesis of bile acids. *Eur. J. Biochem.* **36:** 201–212.
10. Björkhem, I., and J. Gustafsson. 1974. Mitochondrial ω-hydroxylation of cholesterol side chain. *J. Biol. Chem.* **249:** 2528–2535.
11. Setoguchi, T., G. Salen, G. S. Tint, and E. H. Mosbach. 1974. A biochemical abnormality in cerebrotendinous xanthomatosis: Impairment of bile acid synthesis associated with incomplete degradation of the cholesterol side chain. *J. Clin. Invest.* **53:** 1393–1401.
12. Shefer, S., B. Dayal, G. S. Tint, G. Salen, and E. H. Mosbach. 1975. Identification of pentahydroxy bile alcohols in cerebrotendinous xanthomatosis (CTX). Characterization of 5β-cholestane-3α,7α,12α,24ξ,25-pentol and 5β-cholestane-3α,7α,12α,23ξ,25-pentol. *J. Lipid Res.* **16:** 280–286.
13. Björkhem, I., J. Gustafsson, G. Johansson, and B. Persson. 1975. Biosynthesis of bile acids in man. Hydroxylation of the C_{27}-steroid side chain. *J. Clin. Invest.* **55:** 478–486.
14. Salen, G., S. Shefer, G. S. Tint, and E. H. Mosbach. 1975. Role of C_{25}-hydroxy bile alcohols as precursors of cholic acid in man. *Clin. Res.* **23:** 395A.
15. Shefer, S., F. W. Cheng, B. Dayal, S. Hauser, G. S. Tint, G. Salen, and E. H. Mosbach. 1976. A 25-hydroxylation of cholic acid biosynthesis in man and rat. *J. Clin. Invest.* **57:** 897–903.
16. Aringer, L. 1975. Conversion of 7α-hydroxycholesterol and 7α-hydroxy-β-sitosterol to 3α,7α-dihydroxy- and 3α,7α,12α-trihydroxy-5β-steroids in vitro. *J. Lipid Res.* **16:** 426–433.
17. Wyllie, S. G., and C. Djerassi. 1968. Mass spectrometry in structure and stereochemical problems. CXLVI. Mass spectrometric fragmentations typical of sterols with unsaturated side chains. *J. Org. Chem.* **33:** 305–313.
18. Djerassi, C. 1970. Applications of mass spectrometry in the steroid field. *Pure Appl. Chem.* **21:** 205–225.
19. Kihira, K., T. Kuramoto, and T. Hoshita. 1976. New bile alcohols—synthesis of (22*R*)- and (22*S*)-5β-cholestane-3α,7α,12α,22,25-pentols. *Steroids.* **27:** 383–393.
20. Elliott, W. H. 1972. Bile acids. *In* Biochemical Applications of Mass Spectrometry. G. R. Waller, editor. Wiley-Interscience, New York. 291–312.
21. Sjövall, J., P. Eneroth, and R. Ryhage. 1971. Mass spectra of bile acids. *In* The Bile Acids, Vol. 1. P. P. Nair and D. Kritchevsky, editors. Plenum Press, New York. 209–248.
22. Sjövall, J., and K. Sjövall. 1968. Identification of 5α-pregnan-3α,20α,21-triol in human pregnancy plasma. *Steroids.* **12:** 359–366.
23. Suda, T., H. F. DeLuca, H. Schnoes, and J. W. Blount. 1969. 25-Hydroxyergocalciferol: A biologically active metabolite of vitamin D_2. *Biochem. Biophys. Res. Comm.* **35:** 182–185.
24. Morgan, E. D., and C. F. Poole. 1976. The formation of trimethylsilyl ethers of ecdysones. A reappraisal. *J. Chromatogr.* **116:** 333–341.
25. Krasipoel, R. J., N. J. Degenhart, V. Vaabeek, H. De-Leeuw-Boon, G. Abeln, H. K. A. Visser, and J. G. Leferink. 1975. Evidence for 20,22-epoxycholesterol as an intermediate in side-chain cleavage of 22R-OH cholesterol by adrenal cortex mitochondria. *FEBS Lett.* **54:** 172–179.
26. Redel, J., P. A. Bell, N. Bazely, V. Calando, F. Delbarre, and E. Kodicek. 1974. The synthesis and biological activity of 25,26-dihydroxycholecalciferol, a polar metabolite of vitamin D_3. *Steroids.* **24:** 463–476.
27. Ali, S. S., and W. H. Elliott. 1976. Bile Acids LI. Formation of 12α-hydroxyl derivatives and companions from 5α-sterols by rat liver microsomes. *J. Lipid Res.* **17:** 386–392.
28. Kuramoto, T., B. I. Cohen, and E. H. Mosbach. 1976. Isolation, quantitation, and identification of bile alcohols. *Anal. Biochem.* **71:** 481–491.
29. Okuda, K., T. Kuramoto, and T. Kuzano. 1963. Sterobile acids and bile sterols XLI. Isolation of a new bile sterol 3α,7α,12α,25ξ,26-pentahydroxycoprostane from toad bile. *J. Biochem.* **51:** 48–55.
30. McLafferty, F. W. 1963. Decompositions and rearrangements of organic ions. *In* Mass Spectrometry of Organic Ions. F. W. McLafferty, editor. Academic Press, New York. 309–342.
31. Budzikiewicz, H., C. Djerassi, and D. H. Williams. 1967. Mass Spectrometry of Organic Compounds. Holden Day, San Francisco. 21.
32. Dayal, B., A. K. Batta, S. Shefer, G. S. Tint, G. Salen, and E. H. Mosbach. 1978. Preparation of 24(*R*)- and 24(*S*)-5β-cholestane-3α,7α,24-triols and 25(*R*)- and 25(S)-5β-cholestane-3α,7α,26-triols by a hydroboration procedure. *J. Lipid Res.* **19:** 191–196.
33. Dayal, B., S. Shefer, G. S. Tint, G. Salen, and E. H. Mosbach. 1976. Synthesis of 5β-cholestane-3α,7α,12α,25-tetrol and 5β-cholestane-3α,7α,12α,24ξ,25-pentol. *J. Lipid Res.* **17:** 74–77.